

# CHARACTERIZATION OF SILICON CARBIDE PRESSURE SENSORS AT 800 °C

*Robert S. Okojie<sup>1</sup>, Dorothy Lukco<sup>2</sup>, Carl W. Chang<sup>2</sup>, and Ender Savrun<sup>3</sup>*

<sup>1</sup>NASA Glenn Research Center, Cleveland OH 44135 USA

<sup>2</sup>Vantage Partners, LLC, Cleveland OH 44135 USA

<sup>3</sup>Sienna Technologies, Inc., Woodinville WA 98072 USA

## ABSTRACT

Initial characterization of MEMS-based single crystal 4H-SiC piezoresistive pressure sensors has been performed to determine the operational reliability over time at 800 °C. Important parameters such as the zero pressure offset, bridge resistance, and pressure sensitivity as affected by temperature were extracted. These parameters showed relative stability within the prescribed operational window of the sensor at 800 °C. Of significance was the increase in pressure sensitivity with increasing temperature beyond 400 °C, to the extent that the sensitivity at 800 °C equal to or higher than the room temperature value. The sensor can, therefore, be inserted further into the higher temperature section of the test article, thereby making it possible to capture higher frequency bandwidths of the thermoacoustic instabilities, which is critical for the validation of computational fluid dynamics predictive models.

## KEYWORDS

Silicon Carbide, Pressure Sensor, High Temperature, Characterization.

## INTRODUCTION

Pressure sensing in aero-engine and space propulsion combustion chambers is generating increased demand for the purpose of experimental validation of computational fluid dynamics (CFD) codes that are used for engine model predictions prior to production. Currently, there is high uncertainties in these codes, particularly in the high temperature and turbulent regimes. Therefore, experimental validation of these codes is necessary in order to improve their accuracy [1]. It is also desirable to measure in real time the low magnitude pressure transients that are indicative of the onset of thermoacoustic instabilities. Catching these instabilities at low pressure magnitudes makes it easier to mitigate their enlargement and potentially damage critical engine parts [2]. The above stated needs are currently being addressed with state of the art pressure transducers that are traditionally placed at a cooler section several feet away from the combustion chamber to prevent transducer damage while pressure is transmitted from the chamber through semi-infinite tubes. However, the tube length and any distortion in its geometry could result in acoustic reflections and/or attenuation, thus leading to loss of key frequency components or stunt the pressure magnitude [3]. While pressure sensors have been reported to operate at temperatures as high as 800 °C, they were not shown to operate for several hours to assure stable and reliable pressure measurement [4]. A few corporate entities have published datasheets of pressure sensors operating between 700 and 800 °C [5]. However, these piezoelectric

based devices respond only to dynamic pressures. Pressure sensors that simultaneously respond to static and dynamic pressures at high temperature are desirable for effective CFD code validation.

The goal of this work is to develop MEMS based 4H-SiC piezoresistive pressure sensors that could be inserted closer to the combustion chamber of the test article and respond to both static and dynamic pressures. Extending the pressure sensor further toward the combustion chamber would significantly minimize the attenuation of high frequency thermoacoustics that tend to occur when semi-infinite tubes are used. The sensor would capture a wider thermoacoustic frequency bandwidth, thereby providing improved measurements that are required for the accurate validation of the CFD prediction models. This work leverages the previously reported 4H-SiC pressure sensor in which pressure sensitivity was found to increase at 800 °C to levels that were comparable to the pressure sensitivity at room temperature [6]. This work is now extended to characterize the performance of the pressure sensor under constant temperature over time to determine the long term limit of its reliability performance. Key performance parameters were also extracted to determine the level of measurement reliability.

## SENSOR FABRICATION

The starting wafer was a 4-inch diameter, 350 μm thick single crystal semi-insulating 4H-SiC substrate. A 3-μm thick nitrogen doped ( $N_d=2 \times 10^{19} \text{ cm}^{-3}$ ) 4H-SiC layer was homoepitaxially grown by chemical vapor deposition on the substrate Si-face that was tilted 4° off the (0001) basal plane. A 3 μm thick Aluminum (Al) was sputter deposited on the epitaxial layer and Wheatstone bridge configured piezoresistor patterns were defined on it by standard photolithography. This was followed by wet etching of the Al in phosphoric acid (H<sub>3</sub>PO<sub>4</sub>) at 50 °C for 6 minutes. The photoresist was then dissolved in acetone and the patterned Al was used as the etch mask during reactive ion etching (RIE) to transfer the Wheatstone bridge pattern to the epitaxial layer. The epitaxial layer was etched 3.5-μm down to the semi-insulating substrate with the applicable RIE conditions shown in Table 1. The wafer was flipped over to the back side C-face and thin Ni seed layer was deposited on it. This was followed by standard photolithography to define diaphragm patterns. A thicker Ni was then electroplated over the exposed seeded Ni and used as the etch mask. RIE was performed into the semi-insulated substrate, down to the depth that would result in the desired diaphragm thickness. After diaphragm fabrication the residual electroplated Ni was dissolved in a Ni etchant and cleaned in equal volume of H<sub>2</sub>O<sub>2</sub>:H<sub>2</sub>SO<sub>4</sub> for 20 minutes and then rinsed in DI-water.

The wafer was subsequently oxidized at 1150 °C in 6 slpm of flowing ultra-pure oxygen for two hours, after which the grown oxide was stripped off in 49% HF for one minute. This oxidation and stripping process ensured that a pristine epilayer surface was exposed. Next, a 1 μm silicon dioxide layer was sputter deposited on the piezoresistors, followed by photolithography to define the ohmic contact via, which was then etched by RIE. The photoresist was then stripped in acetone, followed by isopropanol dip. Metal deposition followed with the sequential sputter deposition of Ti (100 nm)/TaSi<sub>2</sub> (300 nm)/Ti (1000 nm)/Pt (300 nm). Standard photolithography was applied to define the ohmic contact on the top Pt layer, which was etched in 10:9:1 volume ratio of H<sub>2</sub>O:HCl:HNO<sub>3</sub> for 10 minutes. This was followed by RIE of the underlying metallization for 15 minutes. The residual photoresist was removed by oxygen plasma cleaning process. A rapid thermal anneal (RTA) at 800 °C for 10 seconds in near vacuum was performed to establish the ohmic contact to the SiC piezoresistors. Next was a blanket oxide sputter deposition over the front side, followed by oxide via photolithographic definition and RIE oxide etch that exposed part of the ohmic contact metallization. The residual photoresist was then removed by oxygen plasma clean. Next, a Ti (100 nm)/Pt (300 nm) diffusion barrier layer was deposited, patterned and etched by RIE for 25 minutes. Oxygen plasma clean was performed to remove the residual photoresist.

Table 1: Generic etching recipes for various materials during fabrication.

Material	Etch condition
Metallization	Ar=140 sccm, SF <sub>6</sub> =5 sccm, Power=300 W <sub>rf</sub> , Pressure=25 mTorr.
SiO <sub>2</sub>	SF <sub>6</sub> =15 sccm, Power=100 W <sub>rf</sub> , Pressure=25 mTorr
SiC	Power=400 W <sub>rf</sub> , Ar=25 sccm, SF <sub>6</sub> =15 sccm, pressure=25 mTorr.
Photoresist removal	O <sub>2</sub> =20 sccm, Power=60 W <sub>rf</sub> , Pressure=15 mTorr. 30 minutes.

The above diffusion barrier metal deposition and etching were repeated to obtain a double layer diffusion barrier with a subsequent 10 second RTA, and another quartz deposition, etching, and oxygen plasma clean were performed to open via in the oxide to expose a section of the underlying diffusion barrier layer. Finally, bond pad metallization of TaSi<sub>2</sub> (20 nm)/Pt (100 nm)/Au (1 μm) was deposited. The Au was etched in 10:9:1 volume ratio of H<sub>2</sub>O:HCl:HNO<sub>3</sub> at 40 °C for less than 2 minutes. The TaSi<sub>2</sub>/Pt was etched with the RIE recipe in the above table for the metallization described earlier. After oxygen plasma clean, the wafer was furnace annealed at 700 °C in Ar for 30 minutes, and subsequently diced into individual chips. Finally, thick (~30 μm) Au paste capping layer was applied on each bond pad and cured in the atmospheric oven for 15 minutes at 800 °C.

Known good sensors (KGS) were selected from the diced wafer after confirming the electrical viability of the Wheatstone bridge configured piezoresistors and the uniformity of the diaphragms. These sensors were

packaged based on the MEMS-Direct Chip Attach process [8]. They were then used for pressure and temperature characterization to extract key performance parameters such as pressure and temperature sensitivities, linearity and zero pressure offset (ZPO) voltage drift. A sensor from the unpackaged KGS sub-set was attached to a measurement test fixture and the bond pads were wire bonded with Au wires to the Au pads on the test fixture. The test fixture carrying the sensor was inserted into the atmospheric oven and connected to external wires. Thermal treatment over time was subsequently performed, with intermittent probing of the bridge resistors while at temperature. The ZPO voltage was recorded via digital acquisition over time.

## TEST RESULTS

Only one each of the packaged and unpackaged sensors were tested due to limitations of the test apparatus. The results of the ZPO and bridge resistance of the unpackaged sensor are shown in Figs. 1 and 2, respectively. Both parameters achieved relative stability after the first 100 hours (tentatively defined as the burn-in time) and remained stable for a net total of 170 hours.

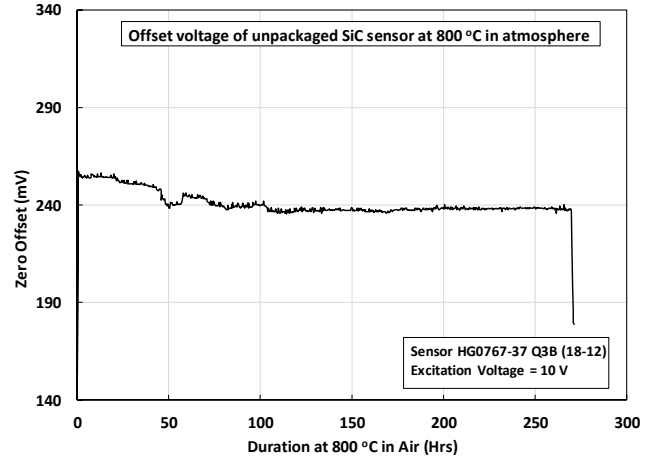


Fig. 1: ZPO of the unpackaged SiC pressure sensor at 800 °C in air.

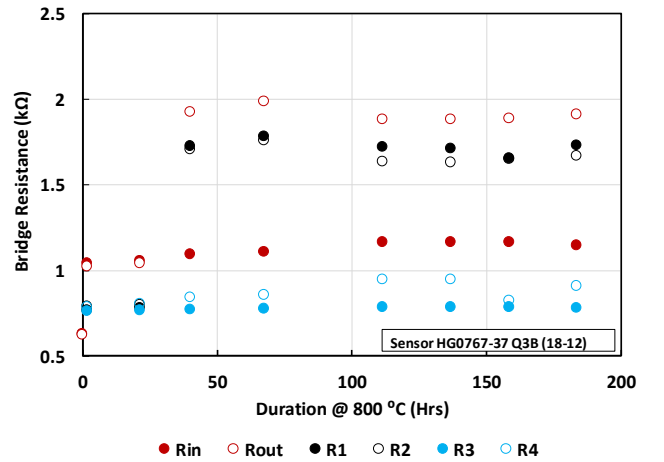


Fig. 2: Bridge resistance of unpackaged SiC pressure sensor during air exposure at 800 °C over time.

Quantitatively, the error band (defined in this case as ZPO maximum and minimum values) during the 170

hours of stability was approximately  $\pm 2.44$  mV of the median value. To evaluate the ZPO of the packaged pressure sensor, it was put through thermal excursion between 400 and 800 °C with no pressure applied, as shown in Fig. 3. Pressure was subsequently applied up to 200 psi at various temperature points up to 800 °C. The net full-scale output (FSO) at 200 psi (i.e., output at 200 psi minus ZPO at that temperature) as function of

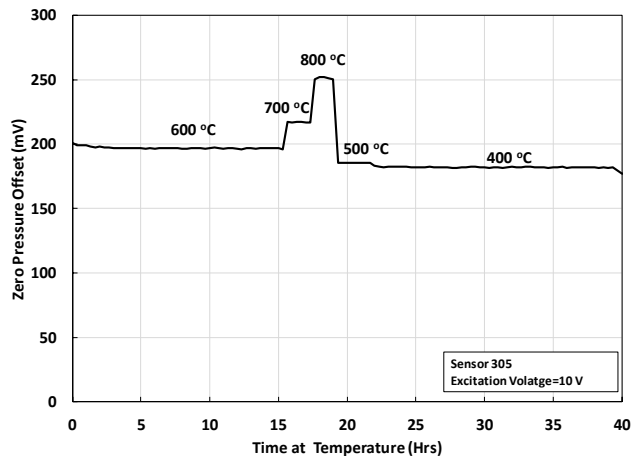


Fig. 3: ZPO of the tested packaged SiC pressure sensor during thermal excursion between 400 and 800 °C.

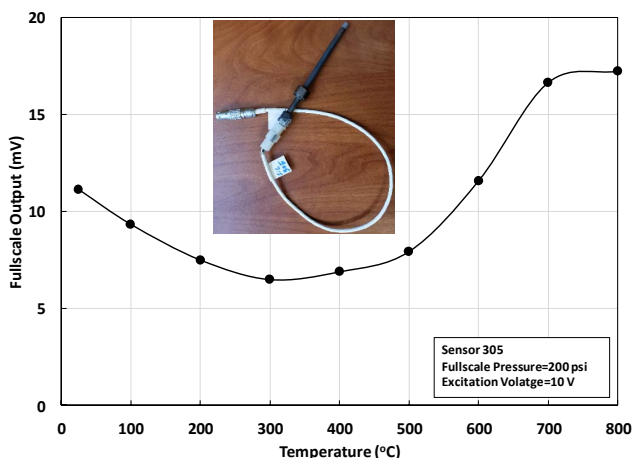


Fig. 4: The FSO of the tested packaged SiC pressure sensor (insert) at selected temperatures.

temperature is shown in Fig. 4. Starting from room temperature the output gradually dropped with increase in temperature. However, an inflection temperature was reached between 300 and 400 °C, beyond which a gradual increase in the net output could be observed. The net output increase continued to 800 °C, at which point it was essentially higher than its room temperature value. This behavior is consistent with the discovery that was reported in [6]. The drop in FSO at 800 °C was due to a leak in the test fixture.

## DISCUSSION

A key parameter that determines the measurement accuracy of a pressure transducer is the stability of its ZPO as a function of temperature from the time of calibration through period of service. The magnitude of ZPO drift from the referenced calibrated value determines

the ZPO drift error band, which is typically expressed as a percentage of the FSO. From Fig. 3, the maximum ZPO drift error band during the course of 1 hour at 800 °C was approximately  $\pm 1.07$  mV, which represented about 6.19 % of FSO (see Fig. 4). Due to the Wheatstone bridge configuration of the sensor, subtle changes in any of the four piezoresistors are manifested as changes in the ZPO voltage. In Fig. 2, the bridge resistance of the unpackaged sensor exhibited some instability during approximately the first 100 hours at 800 °C. This characteristic correlated well with the ZPO drift in Fig. 1 in the first 100 hours, beyond which both resistance and ZPO became stable.

The coupled interaction between the bridge resistance and the ZPO requires an understanding of the fundamental role of the contact metallization (the ohmic contact and diffusion barrier), which is in series with the SiC piezoresistors. After the wafer sensor was annealed in Ar at 700 °C as stated earlier, it was diced into chips. Focused Ion Beam-Field Emission Scanning Electron Microscopy (FIB-FESEM), and Auger Electron Spectroscopy (AES) depth profiling were used to analyze a representative KGS sample, as shown in Figs 5 (a) and (b), respectively. The cross section of the metallization shows evidence of zonal intermetallic mixing within the diffusion barrier and reaction products metal/SiC interface. In Zone 1, the reaction products were primarily

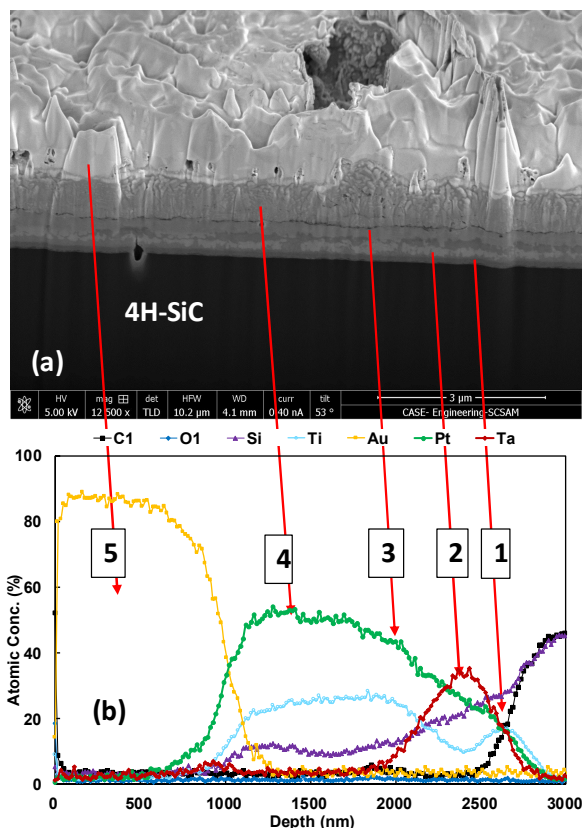


Fig. 5: a) FIB-FESEM cross section image and b) AES depth profile of the ohmic contact metallization and diffusion barrier after Ar anneal at 700 °C for 30 minutes.

silicides and carbides of Ti, which combined to form the ohmic contact on the n-type SiC surface. Zone 2 consisted of silicide complexes of Pt and Ta that functioned as the second layer diffusion barrier. Zones 3 and 4 are the inter-

metallic mixes of Pt/Ti and Pt-rich/Ti to form the first layer diffusion barrier against O from the outer environment and Au from the bond pad and capping layer of Zone 5. The effectiveness of the diffusion barrier scheme in preventing the migration of O and Au to Zone 1 ohmic contact region is key to the overall stability of the bridge resistance, and hence, the

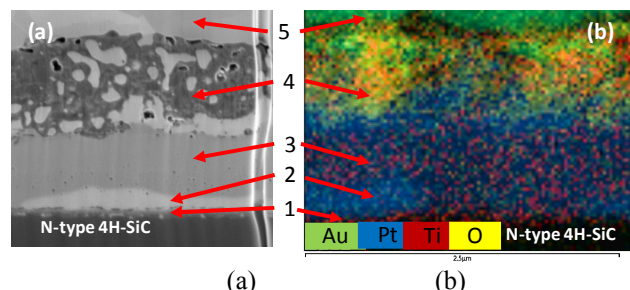


Fig. 6: After 270 hours at 800 °C in air, a) the FIB-FESEM cross section, b) EDS elemental mapping corresponding to the FIB-FESEM image showing the zonal microstructure and elemental distribution.

ZPO. After mounting on a test fixture and tested for 270 hours at 800 °C in air (results shown in Figs. 3 and 4), FIB-FESEM and Energy Dispersive Spectroscopy (EDS) analyses, shown in Fig. 6, were performed for the purpose comparing the changes that had occurred in the metallization and the metal/SiC ohmic contact interface. The AES depth analysis was replaced with EDS due to the inefficiency of AES sputtering through the thick Au capping layer. Elemental mapping by EDS of the FIB cross section of the metallization in Fig. 6 provides an effective method of quantification comparable to AES.

Figures 5 and 6 provide before and after comparisons of the results of thermal activities within the metallization, indicating direct correlation between the ZPO characteristic trend and the microstructural changes as a result of O and Au migration and new reaction products. Some interesting contrasts and similarities were observed. First, the metal/SiC ohmic contact reaction Zone 1 remained largely unperturbed, which would suggest that the changes in the bridge resistance during the 270 hours thermal treatment at 800 °C were not due to changes in ohmic contact resistance. In contrast, significant Pt/Ti intermixing had occurred within Zones 2 and 3, with the former becoming more Pt-rich and agglomerated discontinuously above the ohmic contact of Zone 1. Thermodynamically, the most active was Zone 4, in which Au from the Zone 5 (bond pad and cap) and O from the environment had diffused into the Pt/Ti layer. It can be surmised that the changes in the bridge resistance seen in Fig. 2 during the first 100 hours correlated well with the period during which Au and O were diffusing into the Pt/Ti layer. Both the bridge resistance and the ZPO simultaneously leveled off after the first 100 hours and remained relatively stable for the remaining duration of the test. This would suggest the significant abatement of further Au and O diffusion through the barrier.

It is important to note the characterization described here was based on the exposure of the unpackaged bare 4H-SiC piezoresistive pressure sensor under the most

extreme condition. The fully packaged counterpart sensor like the one shown in the inset of Fig. 4 would have its metallization, resistors, and Au bond pad encapsulated within the package structure. Therefore, only Au would be the primary diffusing element to be concerned about. The packaging used in this test (Fig. 4) was not designed for long duration operation at 800 °C due to oxidation of the braze material. Longer duration operation at that temperature would require some design modification.

## CONCLUSION

The characterization of MEMS-based 4H-SiC piezoresistive pressure sensors, packaged and unpackaged, was performed at 800 °C in air for 1 and 270 hours, respectively. Under the most extreme of test conditions, the unpackaged sensor exhibited good ZPO stability for 170 hours, after the first 100 hours of “burn-in” time. The fully packaged sensor also performed well with low ZPO drift. The significance of this result is that the sensor can now be inserted further into the hotter section of the test article. This would eliminate the use of the traditional semi-infinite tube. Bringing the sensor closer to the sensed environment would capture wider thermoacoustic frequency bandwidth, thereby improving measurement needed for accurate CFD code validation.

## ACKNOWLEDGEMENT

This work was performed in support of the NASA Transformational Tools and Technologies Project. We thank the technicians of the NASA GRC Microfabrication Laboratory for sensor fabrication and Dr. Amir Avishai of Case Western Reserve University, Cleveland, OH, for the elemental analyses.

## REFERENCES:

- [1] W. L. Oberkampf and T. G. Trucano, “Verification and validation in computational fluid dynamics,” *Progress in Aerospace Sciences* 38 (3) 209–272.
- [2] J. J. Keller, “Thermoacoustic oscillations in combustion chambers of gas turbines,” *AIAA Journal*, Vol. 33 (12) (1995), 2280-2287.
- [3] J. A. Spurling, “Using a Semi-Infinite Tube to measure pressure oscillations in solid rocket motors,” *AIAA Propulsion and Energy Forum*, July 27-29, 2015, Orlando, FL, pp. 3976. 2015.
- [4] S. Fricke, A. Friedberg, T. Ziemann, E. Rose, G. Muller, D. Telitschkin, S. Ziegenhagen, H. Seidel, and U. Schmidt, “High temperature (800 °C) MEMS pressure sensor development including reusable packaging for rocket engine applications,” *MNT for Aerospace Applications*, CANEUS, pp. 5p. 2006.
- [5] <https://www.meggitt.com/products-services/pressure-sensors>.
- [6] R. S. Okojie, D. Lukco, V. Nguyen, and E. Savrun, “4H-SiC piezoresistive pressure sensors at 800 °C with observed sensitivity recovery,” *IEEE Electron Device Letters*, Vol. 36 (2), 174-176. 2015.
- [7] US patent US6845664B1.